

A New Method for the Control of Size of Pellets in the Melt Pelletization Process with a High Shear Mixer

Paul Wan Sia HENG,* Tin Wui WONG, Jian Jun SHU, and Lucy Sai Cheong WAN

Department of Pharmacy, National University of Singapore, 10 Kent Ridge Crescent, Singapore 119260.

Received December 1, 1998; accepted January 21, 1999

The control of the melt pelletization process in an 8-l high shear mixer using specific energy consumption of the impeller motor was studied. Lactose was used as the bulk material with polyethylene glycol 3000 as a meltable binder. The effects of binder concentration, mean particle size of bulk material and post-melt impeller speed on the relationship of specific energy consumption and pellet growth were examined. Specific energy consumption was found to be a suitable tool for monitoring the melt pelletization process, and specific energy consumption correlated well with pellet growth. The mean size of the pellets formed becomes correspondingly larger with increasing specific energy consumption. Concerning the impeller speed, specific energy consumption is more useful as a tool for end-point control of the process than post-melt mixing time. Similar size pellets can be obtained with comparable specific energy consumption, independent of the impeller speed. The control of pellet size requires a correlation between pellet growth and specific energy consumption that is established for the formulation and process conditions used. For this purpose, mathematical modelling of the pellet growth process is presented. The predictions of pellet growth by the mathematical model are in agreement with the experimental findings.

Key words high shear mixer; melt pelletization; specific energy consumption; polyethylene glycol; pellet

In conventional wet granulation processes, instrumentation to monitor and control the operation has been studied by several investigators.^{1,2)} The principle of instrumentation involves an indirect measurement that is based upon the changes in the rheological properties of the moist mass that are assumed to be related to the granule growth processes.^{3,4)} Three instrumental methods have been proposed: power consumption,^{1–9)} torque^{1,2,10,11)} and voltage.¹²⁾ Measurement of power consumption and torque are most commonly applied as a tool for process control. Such measurements are performed by means of a power cell and a strain-gauge-based transducer respectively.²⁾ In the wet granulation process, power consumption and torque are used to monitor the quantity of the binder solution to be added and to determine the level of granule growth.

It has been reported that torque generates a more descriptive profile of the granulation process than power consumption. Nevertheless, there are only slight differences in the suitability of these methods for process monitoring purposes.^{1,2)} For process control in the granulation operation, the measurement of power consumption is indeed considered to be more practical due to its simplicity, reliability and low cost.^{2,3)} It appears that this measurement is preferable even when compared with the direct measurement of granule growth using a video imaging system and moisture determination using an infrared moisture sensor in the fluidized bed granulation process.^{13,14)} In granulation equipment such as a high shear mixer, control of granule growth by direct imaging is extremely difficult to perform.

The measurement of power consumption has been reported for the control of pellet growth in the melt pelletization process, although it was found to be limited in application.^{15–17)} The reason reported is that the deformability of agglomerates containing a non-aqueous molten binder was relatively low in comparison to that of agglomerates formed using an aqueous binding liquid. The measurement of power consumption was reported to be not sufficiently sensitive to

reflect the small changes in the deformability of melt agglomerates associated with pellet growth, except when the impeller speed was high.¹⁸⁾ This paper reports investigations to apply a new method for modelling pellet growth in melt pelletization, based upon the measurement of energy consumption.

Experimental

Materials Lactose (α -monohydrate lactose, Pharmatose, DMV, The Netherlands) 200, 350 and 450 M with mean particle sizes of 40.32, 35.58 and 21.11 μm respectively were used as the bulk materials with polyethylene glycol 3000 (PEG 3000, Hoechst, Germany) of mean particle size 34 μm as binder. Particle sizes were determined using a laser diffracting particle sizer (Malvern, 2600c with dry powder feeder, U.K.). The melting point of PEG 3000 is 59.5–62.7 °C (capillary method, Gallenkamp, U.K.).

Equipment A laboratory scale vertical high shear mixer (Pellmix PL 1/8, Niro, Denmark) not fitted with a chopper, was used for preparation of the pellets. The mixer was water-jacketed for cooling and heating. The inner wall was polytetrafluoroethylene (PTFE)-lined. The mixer was fitted with a conical PTFE lid with a viewing glass port at the truncated apex.

A two-bladed, bottom-driven impeller with speeds adjustable up to 1500 rpm was used. The tips of these impeller blades were curved. The bowl was equipped with a thermoresistance probe (PT 100), allowing the temperature of the product to be recorded. The probe was placed in the side wall of the bowl, 50 mm from the floor of the mixer.

Preparation of Pellets In the pelletization of lactose 450 M, a load of lactose (1 kg) and PEG 3000 at concentration levels of 22, 23 and 24% (w/w), expressed as the percentage of lactose, was used. This amount of PEG 3000 was reduced to 17% (w/w) when a study was carried out to compare the use of lactose 200, 350 and 450 M. The lactose and binder were first manually mixed in a plastic bag for 5 min. The mixture was then transferred to the high shear mixer and mixed at an impeller speed of 1300 rpm. Outputs for power consumption, product temperature and impeller speed were recorded using a 3-pen recorder (LR92620, Linear, U.S.A.). During the dry-mixing phase, the high impeller speed produces shear friction that increases the product temperature to the melting point of the binder within a reasonably short time. The onset of melting is read at the inflection point on the product temperature-mixing time profile of the recorder tracing. The pre-melt mixing time was taken from the start of high shear mixing in the melt pelletizer to the onset of binder melting. The post-melt mixing time was the additional process time taken from the onset of binder melt to the end of the run. At 2 min after onset of melting, the impeller speed was reduced to 1150 rpm, unless otherwise stated.¹⁹⁾

* To whom correspondence should be addressed.

At the start of each run, the water jacketed bowl was maintained at 30 °C. This low temperature prevents premature binder melting. One minute into the post-melt mixing, the jacket set temperature was increased to 80 °C. A higher temperature reduces material adhesion. On completion of a run, the pellets were immediately collected, weighed and then spread out in thin layers on trays to cool. For each variable studied, preparation of pellets was carried out with a different post-melt mixing time.

Size Analysis The pellets from each run were randomly divided using a sampler (Retsch, PT, Germany). A sample of about 100 g was sized using a nest of sieves of aperture sizes 1, 1.4, 2 and 2.8 mm, at an amplitude of 1 mm (Endecotts, EVS1, U.K.) for 10 min. The sample collected in the receiving pan was subsequently transferred to another set of sieves of sizes 0.075, 0.125, 0.25, 0.355, 0.5 and 0.71 mm and vibrated for 20 min. The mean size of pellets (d_{gw}) was calculated using equation described by Schaefer and Worts.²⁰⁾

$$\log d_{gw} = \frac{\sum w_i \cdot \log d_i}{\sum w_i} \quad (1)$$

where d_i is the mean diameter and w_i is the weight of pellets, of sieve fraction i .

Results

From Fig. 1, it can be seen that the mixing process is divided into two phases: pre- and post-melt mixing phases. The power consumption of the impeller motor is low and almost constant during the pre-melt mixing phase, but increases markedly only when the binder begins to melt. This behaviour may be explained with reference to the melting process of the binder. Once melted, the molten binder converts the powder into a cohesive mass, giving rise to the greater resistance experienced by the impeller. This resistance is reduced as the larger cohesive mass breaks down into small irregular primary agglomerates. From around 15 min into the post-melt phase, a small rise in resistance can be detected by increased power consumption. This may be associated with an increase in the product temperature which results from some release of moisture or water of crystallization from the lactose bulk material.

In the post-melt mixing phase, the process of pellet formation begins. Since power consumption is thought to reflect the stage of development of the product, it may be useful to apply this measurement to the search for a means to determine the end-point of the process. The post-melt power consumption, P_{sum} , is a composite of three components, P_{idle} , P_{mix} , and P_{melt} . P_{idle} is the power component of impeller rotation in the absence of powder material and P_{mix} is the component equivalent to the relatively constant power fraction during the pre-melt mixing phase at the same impeller speed. P_{melt} is the additional power consumed during the post-melt mixing phase. For modelling, the post-melt power consumed, P_t refers to P_{melt} . Three physical derivatives are taken from the profiles of post-melt power consumption vs. mixing time. These are:

1. Post-melt specific power consumption taken at specified time, P_t'' . This is obtained by normalising the post-melt power consumption, P_t , read at the specified post-melt mixing time t , with the total mass of powder, M , used.

$$P_t'' = \frac{P_t}{M} \quad (2)$$

2. Post-melt specific energy consumption, E_{melt} . This is obtained by integrating the area under the post-melt specific power consumption vs. mixing time curve.

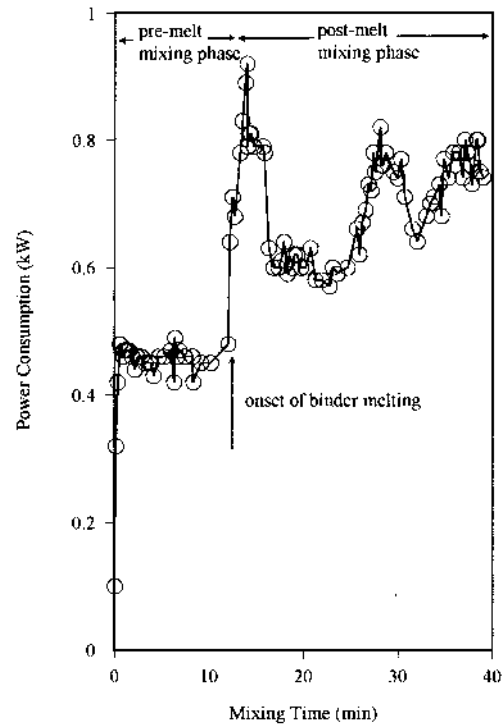


Fig. 1. Profile of Power Consumption at Pre-Melt and Post-Melting Phases

Material: lactose 450 M; PEG 3000 concentration: 23%; pre-melt impeller speed: 1300 rpm; post-melt impeller speed: 1150 rpm.

$$E_{melt} = \int_0^t P_t'' \quad (3)$$

3. Average post-melt specific power consumption, P_{av} . This represents the quotient of post-melt specific energy consumption and the corresponding length of mixing time.

$$P_{av} = \frac{\int_0^t P_t''}{t} \quad (4)$$

The normalized derived values, P_t'' , P_{av} and E_{melt} are plotted against the mean size of pellets formed from lactose 450 M. The relationships are examined for pellets formed at different post-melt mixing time. Overall, it is observed that variation of mean pellet size with E_{melt} is closer to linear correlation than that in P_t'' or P_{av} at all binder concentrations considered (Table 1). This is because the specific energy consumption is considered as the amount of work input for the formative process of consolidating the powder mass into pellets. It is more indicative of the stage of pellet growth.

With reference to Eq. 3, the control of mean pellet size by post-melt specific energy consumption is basically a time determination of the process end-point. It is evident from Fig. 2 that E_{melt} and post-melt mixing time are linearly correlated and formation of larger pellets at longer processing time involves a greater level of E_{melt} . Nevertheless, E_{melt} is found to be more useful as a tool for control of pellet growth where post-melt impeller speed is varied. Figure 3 shows that its relationship with mean pellet sizes at different post-melt mixing times is independent of the effects of post-melt impeller speed and a linear relationship between E_{melt} and mean pellet

Table 1. Correlation Study on the Relationship of Mean Pellet Size with Post-Melt Specific Power and Energy Consumption

PEG 3000 concentration (%)	Post-melt mixing time (min)	Mean pellet size (μm)	Correlation coefficient of mean pellet size with		
			P_r''	P_{av}	E_{melt}
22	5	391.71	0.7750	0.7350	0.9970**
	9	474.89			
	13	579.07			
	17	669.59			
	21	754.37			
23	25	892.18	0.7400	0.5200	0.9840**
	5	453.34			
	9	522.95			
	13	703.94			
	17	866.25			
24	21	937.84	0.9140*	0.8430*	0.9780**
	25	1092.32			
	5	609.47			
	9	740.83			
	13	1142.68			
	17	1212.86			
	21	1339.49			
	25	1878.42			

Bulk material: lactose 450 M; post-melt impeller speed: 1150 rpm. * At 0.05 level of significance. ** At 0.01 level of significance.

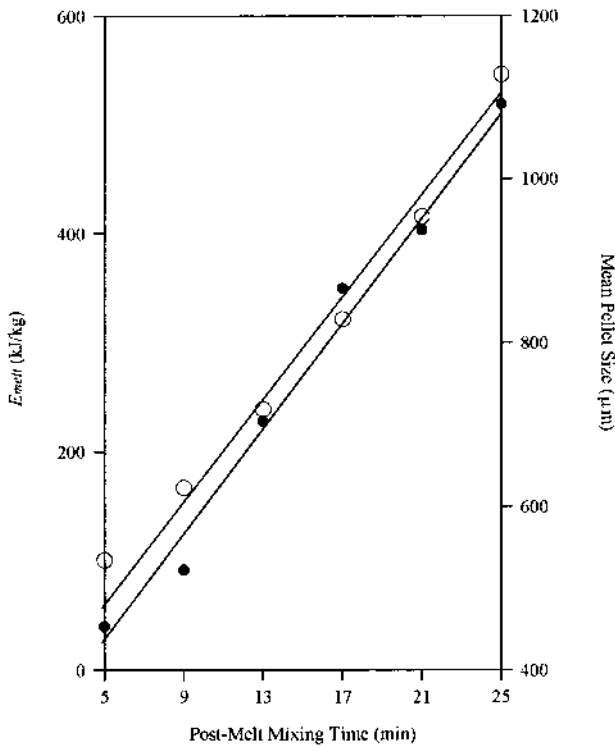


Fig. 2. Relationships of Post-Melt Specific Energy Consumption, E_{melt} , and Mean Pellet Size with Post-Melt Mixing Time

Material: lactose 450 M; PEG 3000 concentration: 23%; post-melt impeller speed: 1150 rpm. E_{melt} , \circ ; mean pellet size, \bullet .

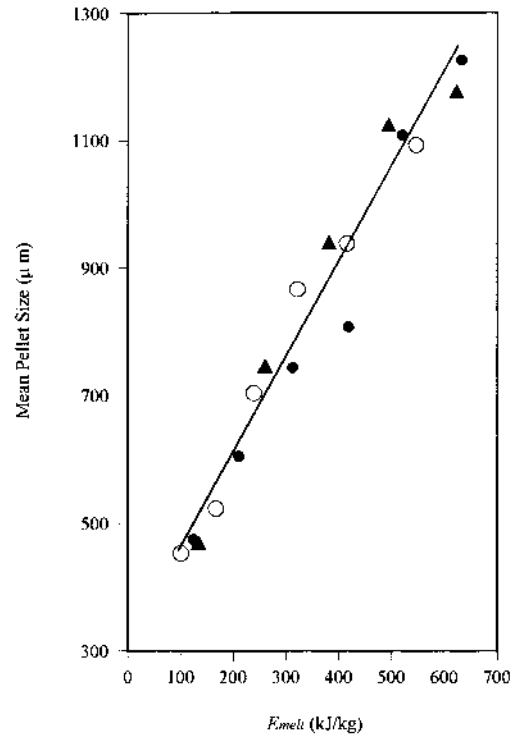


Fig. 3. Relationship of Post-Melt Specific Energy Consumption, E_{melt} , and Mean Size of Pellets Formed at Different Post-Melt Mixing Time with Respect to the Effect of Post-Melt Impeller Speed (Correlation Coefficient: 0.9587)

Material: lactose 450 M; PEG 3000 concentration: 23%; post-melt impeller speed (rpm): \circ , 1150; \bullet , 1300; \blacktriangle , 1450.

size is found. Similar size pellets can be obtained with comparable E_{melt} in processes where different post-melt impeller speeds are used. This is because the variation of impeller speeds affects E_{melt} which in turn, controls pellet growth.

However, the E_{melt} -pellet size relationship established is found to be affected by binder concentration and bulk material used. In pelletization of lactose 450 M using different levels of binder at a post-melt impeller speed of 1150 rpm, it is

found that the pellets grow larger at higher binder level while E_{melt} remains insensitive to the changes in the binder concentration (Fig. 4). Similarly, the rate of pellet growth varies with the particle size of the lactose bulk material, though the level of post-melt specific energy consumption is comparable among the processes using different size grades of lactose bulk material (Fig. 5). The reason for this is that for the pro-

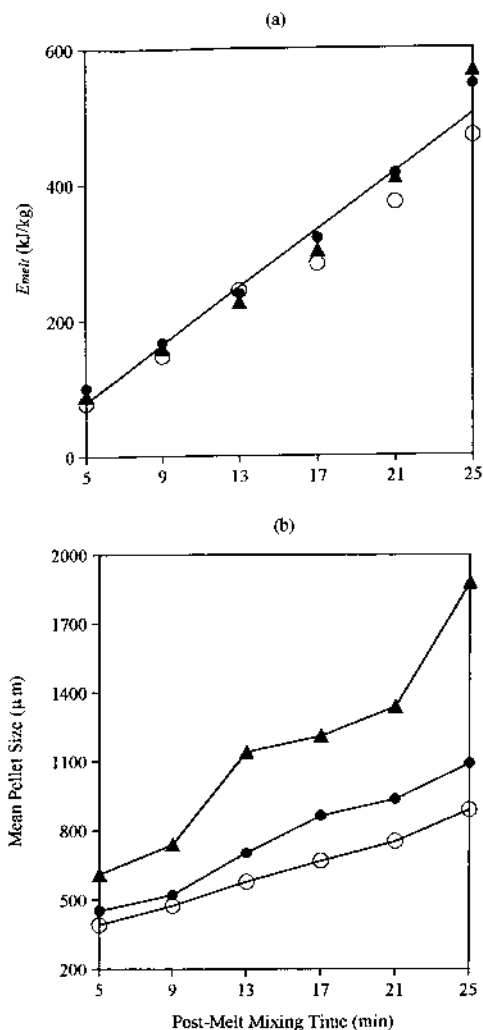


Fig. 4. Profiles of (a) Post-Melt Specific Energy Consumption, E_{melt} , and (b) Mean Size of Pellets Formed at Different Post-Melt Mixing Time with Respect to the Effect of Binder Concentration

Material: lactose 450M; post-melt impeller speed: 1150 rpm; PEG 3000 concentration (%): \circ , 22; \bullet , 23; \blacktriangle , 24.

duction of melt pellets, the variations in binder concentration and particle size of bulk material are within narrow ranges. Thus, the general growth process of pellets can be described by the energy consumed, and changes in the binder concentration and particle size of bulk material show minimal influence. The control of pellet growth requires a relationship that includes the effects caused by binder concentration and bulk material. Formation of larger pellets at higher binder concentration is merely a consequence of the rise in the amount of binder for agglomeration. It is not related to the specific energy consumption of the process. The specific energy consumption of the pelletization run remains largely unchanged. At each time, no differences in E_{melt} are found though the mean size of the pellets is larger with the use of a greater amount of PEG. Similarly, differences in pellet growth associated with changes in the particle sizes of the bulk material do not appear to be related to E_{melt} . The difference in the growth profile of coarser material from finer particles is independent of the post-melt specific energy consumption. It is due to the differences in the agglomerative potential of the powder material. The coarser material has smaller specific

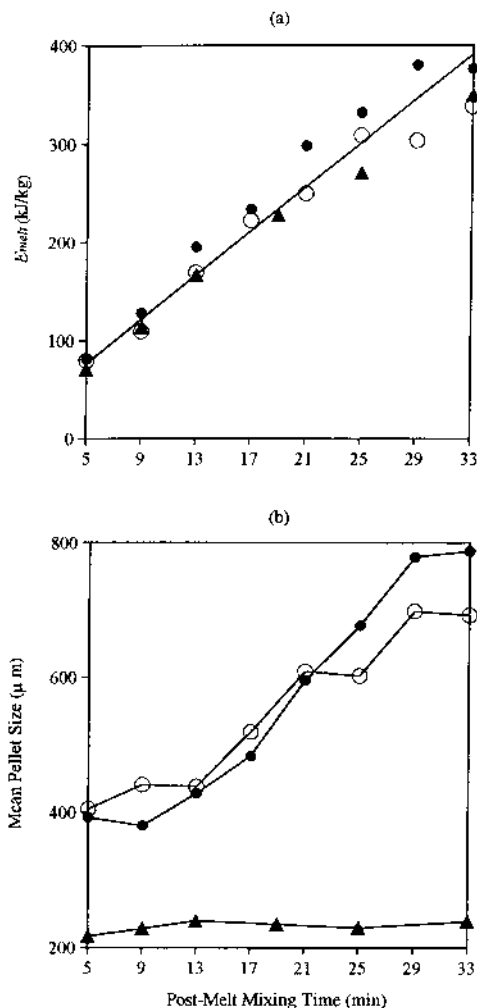


Fig. 5. Profiles of (a) Post-Melt Specific Energy Consumption, E_{melt} , and (b) Mean Size of Pellets Formed at Different Post-Melt Mixing Time with Respect to the Effect of the Particle Size of Bulk Material

PEG 3000 concentration: 17%; post-melt impeller speed: 1150 rpm; lactose mesh size (μm): \circ , 200; \bullet , 350; \blacktriangle , 450.

particle surface area. It requires a lower binder concentration than lactose 450M in making pellets with the same mean size. From Fig. 5, it is shown that there is no significant increase in the mean size of lactose 450M pellets prepared using 17% of PEG with post-melt mixing time. In the case that power consumption is more or less constant in the post-melt mixing phase, the energy consumption increases linearly with the post-melt mixing time. From the experimental results in the majority of cases, a further increase in the mean pellet size with post-melt mixing time is found because a sufficient amount of binder is used (Figs. 4, 5). This may be related to the fact that the surface of pellets is sufficiently wetted for further growth, which does not seem to be the case for the fine lactose 450M when 17% of PEG is used according to Fig. 5.

In the process of melt pelletization, the post-melt specific energy consumption is well correlated with pellet growth. It is found to be more suitable and convenient for use in end-point control of the pelletization process. However, the effects of binder concentration and particle size of the bulk material need to be taken into consideration when E_{melt} is

used. For this purpose, an attempt to form an equation by mathematical modelling relating the pellet size with the process and formulation parameters was carried out. This was aimed at establishing a common relationship that can be used when adjustments are made to the formulations or process variables.

Mathematical Modelling Since pelletization results from direct interactions between discrete particles, the processes of pellet formation and growth can be appropriately described in terms of macroscopic population balance models. The discrete form of the population balance can be expressed by the Smoluchowski equation²¹⁾

$$\frac{dn_k(t)}{dt} = \frac{\lambda}{2N^\alpha(t)} \sum_{l=1}^{k-1} n_l(t)n_{k-l}(t) - \frac{\lambda}{N^\alpha(t)} n_k(t) \sum_{l=1}^{\infty} n_l(t) \quad (5)$$

with the initial condition $n_k(0) = \begin{cases} N(0) & k=1 \\ 0 & k>1 \end{cases}$ where $n_k(t)$ is the

number density of pellets of size k , at post-melt mixing time t , λ is the pelletization kernel, $0 < \alpha < 1$ ($\alpha=0$ for dilute systems and $\alpha=1$ for concentrated systems) and the total number of particles at time t , $N(t)$, is given by

$$N(t) = \sum_{l=1}^{\infty} n_l(t) \quad (6)$$

Summation of Eq. 5 from $k=1$ to ∞ yields:

$$\frac{dN}{dt} = -\frac{\lambda}{2} N^{2-\alpha} \quad (7)$$

It is valuable to introduce the following transformation variables:

$$\theta = \frac{N(t)}{N(0)}, \quad f_k(\theta) = \frac{n_k(t)}{N(t)} \quad (8)$$

where $f_k(\theta)$ represents the number fraction of the species of size k , at dimensionless time θ .

Introducing the variables defined by Eq. 8 into Eq. 5, and using Eq. 7, a modified coalescence rate equation is obtained:

$$\theta \frac{df_k}{d\theta} = f_k - \sum_{l=1}^{k-1} f_l f_{k-l} \quad (9)$$

with the initial condition

$$f_k(1) = \begin{cases} 1 & k=1 \\ 0 & k>1 \end{cases}$$

Eq. 9 can be solved by generation function techniques.²²⁾ It is given by

$$f_k(\theta) = \theta(1-\theta)^{k-1} \quad (10)$$

The relative pellet size \bar{k} can be defined by

$$\bar{k} = \frac{\sum_{k=1}^{\infty} k n_k(t)}{N(t)} = \sum_{k=1}^{\infty} k f_k(\theta) = \theta \sum_{k=1}^{\infty} k(1-\theta)^{k-1} = \frac{1}{\theta} \quad (11)$$

Therefore, using Eq. 7, Eq. 11 can be rewritten:

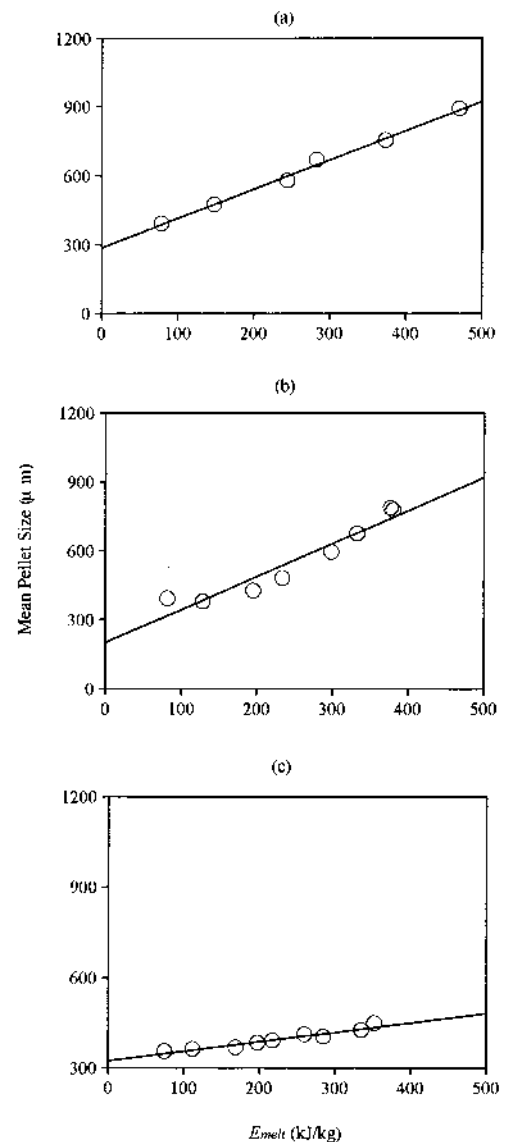


Fig. 6. Profiles of Predicted (—) and Experimental (○) Relationships between Post-Melt Specific Energy Consumption, E_{melt} , and Mean Size of the Pellets Formed at Different Post-Melt Mixing Time

Lactose mesh size (M)/PEG 3000 concentration (%): (a) 450/22; (b) 350/17; (c) 200/16.

$$d = d_0 \left[1 + \frac{\lambda(1-\alpha)N^{1-\alpha}(0)}{2} t \right]^{\frac{1}{3(1-\alpha)}} \quad (12)$$

where d is the mean pellet size at time t , and d_0 is the initially monosized particle size of bulk material. The post-melt specific energy consumption E_{melt} is directly proportional to post-melt mixing time t , regardless of binder concentration c , and particle size s , of bulk material (Figs. 4a, 5a). The value of α is determined by the concentration of a system. For melt pelletization data, it is estimated that $\alpha=2/3$ via curve estimation. The model of melt pelletization considered here can be summarized by

$$d = f_1(s)[1 + f_2(c)E_{melt}] \quad (13)$$

Using a curve estimation technique, examples of parameters calculated are

$$f_1(s) = 1661.54 - 100.210s + 1.6634s^2$$

$$f_2(c) = -0.4001 + 4.2878c - 11.132c^2 \quad (14)$$

when $s = 21.11 \mu\text{m}$ and $c = 22\%$, $s = 35.58 \mu\text{m}$ and $c = 17\%$, or $s = 40.32 \mu\text{m}$ and $c = 16\%$.

Figure 6 illustrates that the results predicted by Eq. 13 with Eq. 14 are in good agreement with the experimental data for various binder concentrations and particle sizes of bulk material.

Conclusions

Post-melt specific energy consumption is found to be suitable for use in the end-point control of the melt pelletization process. It is more accurate as a tool for process control when compared to the post-melt power consumption. In the mathematical modelling of the pelletization process using E_{melt} instead of post-melt mixing time as an end-point determinant, a lower number of process variables needs to be taken into consideration where the relationship of E_{melt} and pellet size is established. A more descriptive profile of the level of pellet growth can be performed with the use of E_{melt} in control of the melt pelletization process, as it gives an indication of the work load required to consolidate the powder mass into pellets.

References

- 1) Corvari V., Fry W. C., Seibert W. L., Augsburg L., *Pharm. Res.*, **9**, 1525—1533 (1992).
- 2) Kopcha M., Roland E., Bubb G., Vadino W. A., *Drug Dev. Ind. Pharm.*, **18**, 1945—1968 (1992).
- 3) Holm P., Schaefer T., Kristensen H. G., *Powder Technol.*, **43**, 225—233 (1985).
- 4) Leuenberger H., *Pharm. Acta Helv.*, **57**, 72—82 (1982).
- 5) Ritala M., Jungersen O., Holm P., Schaefer T., Kristensen H. G., *Drug Dev. Ind. Pharm.*, **12**, 1685—1700 (1986).
- 6) Ritala M., Holm P., Schaefer T., Kristensen H. G., *Drug Dev. Ind. Pharm.*, **14**, 1041—1060 (1988).
- 7) Shiraishi T., Kondo S., Yuasa H., Kanaya Y., *Chem. Pharm. Bull.*, **42**, 932—936 (1994).
- 8) Shiraishi T., Sano A., Kondo S., Yuasa H., Kanaya Y., *Chem. Pharm. Bull.*, **43**, 654—659 (1995).
- 9) Shiraishi T., Yaguchi Y., Kondo S., Yuasa H., Kanaya Y., *Chem. Pharm. Bull.*, **45**, 1312—1316 (1997).
- 10) Lindberg N. O., *Acta Pharm. Suec.*, **14**, 197—204 (1977).
- 11) Tapper G. I., Lindberg N. O., *Acta Pharm. Suec.*, **23**, 47—56 (1986).
- 12) D'Alonzo G. D., O'Connor R. E., Schwartz J. B., *Drug Dev. Ind. Pharm.*, **16**, 1931—1944 (1990).
- 13) Watano S., Miyanami K., *Powder Technol.*, **83**, 55—60 (1995).
- 14) Watano S., Terashita K., Miyanami K., *Chem. Pharm. Bull.*, **39**, 1013—1017 (1991).
- 15) Schaefer T., Holm P., Kristensen H. G., *Acta Pharm. Nord.*, **4**, 141—148 (1992).
- 16) Schaefer T., Holm P., Kristensen H. G., *Acta Pharm. Nord.*, **4**, 245—252 (1992).
- 17) Royce A., Suryawanshi J., Shah U., Vishnupad K., *Drug Dev. Ind. Pharm.*, **22**, 917—924 (1996).
- 18) Schaefer T., Thesis on Melt Agglomeration, Copenhagen, 1996.
- 19) Heng P. W. S., Wan L. S. C., Wong T. W., *Pharm. Dev. Technol.* in press.
- 20) Schaefer T., Wörts O., *Arch. Pharm. Chem. Sci.*, **5**, 51—60 (1977).
- 21) Smoluchowski M. V., *Physik. Z.*, **17**, 557—571, 585—599 (1916).
- 22) Bharucha-Reid A. T., "Elements of the Theory of Markov Processes and Their Applications," McGraw-Hill Book Company, Inc., New York, 1960.